DALTON
FULL PAPER

Structural and mechanistic information on the reaction of bicarbonate with Cu(II) and Zn(II) complexes of tris(2-aminoethyl)amine. Identification of intermediate and product species

Zong-Wan Mao,† Günter Liehr and Rudi van Eldik *

Institute for Inorganic Chemistry, University of Erlangen-Nürnberg, Egerlandstr. 1, 91058 Erlangen, Germany. E-mail: vaneldik@chemie.uni-erlangen.de

Received 3rd January 2001, Accepted 30th March 2001
First published as an Advance Article on the web 30th April 2001

A series of binuclear bicarbonato, trinuclear carbonato and binuclear hydroxo complexes were isolated in the reaction of $[M(tren)(H_2O)](ClO_4)_2$ (M = Cu(II), Zn(II) and tren = tris(2-aminoethyl)amine) with $NaHCO_3$ at pH *ca.* 6.5, 8.5 and 10.0, respectively, and physically characterized. The structures of two trinuclear carbonato complexes, $\{[Cu(tren)]_3(\mu_3\text{-}CO_3)\}(ClO_4)_4\cdot H_2O$ and $\{[Zn(tren)]_3(\mu_3\text{-}CO_3)\}(ClO_4)_4\cdot H_2O$ were determined by X-ray analysis. UV-Vis spectra of $[Cu(tren)(H_2O)](ClO_4)_2$ were recorded as a function of pH in the absence and presence of $NaHCO_3$, and reveal evidence for a carbonation process in the pH range 6.0 to 9.5 and a hydrolysis process in the range pH 9.5 to 12. ^{13}C NMR measurements on $[Zn(tren)(H_2O)](ClO_4)_2$ as a function of pH in the presence of $NaH^{13}CO_3$, indicated that the Zn(II) complex behaves similarly to the Cu(II) complex in solution, and that the polynuclear carbonato complexes are only formed at low concentrations in solution. The kinetics of the reaction of $[Cu(tren)(H_2O)]^{2+}$ with HCO_3^- was studied by stopped-flow using a pH-jump technique. The results indicated that complex-formation of $[Cu(tren)(H_2O)]^{2+}$ with HCO_3^- is too fast to be resolved kinetically. The observed kinetics and second-order rate constant of $494 \pm 10\ M^{-1}\ s^{-1}$ were assigned to the rate-determining formation of a binuclear carbonato complex. A plausible mechanism for the carbonation of CuN_4 complexes that include an axial water molecule in a trigonal bipyramidal structure, is proposed.

Introduction

The reversible hydration of carbon dioxide and dehydration of bicarbonate catalyzed by carbonic anhydrase as shown in eqn. (1), has aroused much interest over the years.[1] Both the

$$CO_2 + H_2O \rightleftharpoons HCO_3^- + H^+ \qquad (1)$$

nature of the active site and the catalytic mechanism have been addressed by numerous experimental and theoretical studies.[2] The structures of several forms of the enzyme have been determined by X-ray diffraction. In human carbonic anhydrase II,[3] the active site contains a pseudo-tetrahedral zinc center coordinated to three histidine imidazole groups and a water molecule or hydroxide anion, depending on the pH ($pK_a \approx 7$). The active site is connected to a network of hydrogen bonds formed by adjacent residues and water molecules. It has been widely accepted that the R_3Zn–OH form of the enzyme is the active species in the hydration of CO_2, whereas the R_3Zn–H_2O form is the active species in the dehydration of HCO_3^-. The reversible mechanism to account for the catalytic activity of carbonic anhydrase can in general be summarized as in Scheme 1.[1]

In various approaches, many model compounds were synthesized and the kinetic behavior of some of these complexes was studied for the reaction with CO_2/HCO_3^-.[4–20] The results clearly indicated that the hydroxo form of the metal complexes is the active species for CO_2 uptake. In our earlier work, we have performed detailed kinetic studies on the hydration and dehydration reactions of two model complexes,[11b,c] and found that the measurements for the dehydration reaction were affected by the reverse hydration process. Since these Zn(II) ions and their complexes are spectroscopically inactive in the UV-Vis range, the kinetics of the reaction could only be monitored indirectly *via* a pH-indicator-buffer method, which was developed for the study of the enzyme and model complexes.[2b] In this method complications may occur due to the co-existence of other acid–base equilibria in solution, and even result in inappropriate conclusions. Therefore, an alternative approach would be to replace Zn(II) by a UV-Vis active metal ion such as Cu(II), as a probe for the kinetic studies.

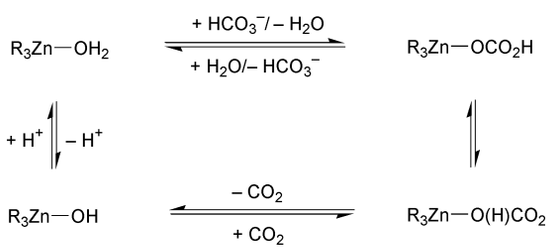

Scheme 1 The overall proposed catalytic mechanism for the carbonic anhydrase enzyme.

Using Cu(II) ion as a probe in carbonic anhydrase may introduce another complication, since Cu(II)-substituted carbonic anhydrase only showed little residual activity.[21] Two possible explanations for the behavior of Cu(II) in the enzyme have been offered. One is that the Cu(II)-substituted carbonic anhydrase does not react with CO_2/HCO_3^- at all, although it was found that some Cu(II) hydroxo complexes are very effective towards CO_2 uptake and for a variety of hydrolytic reactions.[10,22]

† On leave from School of Chemistry and Chemical Engineering, Zhongshan University, 510275 Guangzhou, P.R. China.

DOI: 10.1039/b100160o

Another is that the Cu(II) ion can easily form a bidentate bicarbonate intermediate, with the result that bicarbonate is tightly bound and does not participate effectively in the further catalytic cycle.[10] Model studies on monomeric nitrate and binuclear carbonato complexes revealed the preference for bidentate coordination in going from Zn(II) to Cu(II). However, theoretical calculations indicated that the stable bidentate bicarbonate intermediate is favorable for proton transfer in the catalytic cycle.[2d] In addition, the structures of a monodentate bicarbonato complex of a non-native mutant of HCAII (Thr-200→His-200) and an approximate bidentate bicarbonato complex of HCAI, have been determined. The metal ion–bicarbonate distances are between 1.8 and 3.5 Å in the former, and between 2.2 and 2.5 Å in the latter case.[23,24] Thus the reason for the lower activity of the Cu(II)-substituted carbonic anhydrase remains to be resolved.

In order to further probe the dehydration mechanism of the active center of the enzyme, as well as the relevance of the Cu(II) geometry for the catalytic activity, our recent investigations focused on the kinetics of the reactions of a few Cu(II) complexes with HCO_3^-, as well as on the reaction behavior of the corresponding Zn(II) complexes with HCO_3^-. First, the copper and zinc complexes of tris(2-aminoethyl)amine (tren) were selected, which adopt a trigonal bipyramidal geometry with a coordinated H_2O molecule located in the axial position. To confirm the nature of the overall reaction process, the necessary intermediates and products were isolated and structurally characterized. Here we also report a mechanistic study of the reaction of $[Cu(tren)(H_2O)]^{2+}$ with HCO_3^-, as well as the preparation and structures of polynuclear carbonato complexes. A plausible reaction mechanism is suggested.

Experimental

Materials

All metal salts were of analytical reagent grade and used without further purification. The tren ligand was purchased from Sigma. The complexes, $[Cu(tren)(H_2O)](ClO_4)_2$ and $[Zn(tren)(H_2O)](ClO_4)_2$, were prepared and characterized according to the literature method.[25] $NaHCO_3$ was obtained from Fluka and $NaH^{13}CO_3$ from Aldrich.

Syntheses

$\{[Cu(tren)]_3(\mu_3\text{-}CO_3)\}(ClO_4)_4\cdot H_2O$ (1). A mixture of 0.408 g (1.0 mmol) of $[Cu(tren)(H_2O)](ClO_4)_2$ and 0.084 g (1.0 mmol) of $NaHCO_3$ were dissolved in 20 mL of water and stirred for 5 min at room temperature and a pH between 8 and 9. The solution was filtered and allowed to stand in a desiccator with P_2O_5 for slow evaporation. After a few days, 0.203 g (55.1%) of blue block crystals was obtained, suitable for X-ray analysis. IR cm^{-1} (KBr pellet): 3298s, 2929m, 1599m, 1459s, 1389w, 1361w, 1308m, 1286w, 1264m, 1110s, 902m, 838m, 746m, 627s. Anal. Calcd for $C_{19}H_{56}N_{12}Cl_4O_{20}Cu_3$: C, 20.65; H, 5.11; N, 15.21. Found: C, 20.93; H, 5.07; N, 15.45%.

$\{[Cu(tren)]_2(\mu\text{-}CO_3H)\}(ClO_4)_3\cdot H_2O$ (2). A mixture of 0.408 g (1.0 mmol) of $[Cu(tren)(H_2O)](ClO_4)_2$ and 0.252 g (3.0 mmol) of $NaHCO_3$ were dissolved in 20 mL of water and then $HClO_4$ was added slowly to adjust the pH value to *ca.* 6.0. The solution was filtered and allowed to stand in a desiccator with P_2O_5 under CO_2 atmosphere for slow evaporation. After a few days, 0.075 g (18.8%) of pale blue fine needle crystals was obtained. IR cm^{-1} (KBr pellet): 3260s, 2931m, 1596m, 1462s, 1440s, 1395w, 1372w, 1362w, 1308m, 1115s, 902m, 840m, 746m, 626s. Anal. Calcd for $C_{13}H_{39}N_8Cl_3O_{16}Cu_2$: C, 19.59; H, 4.93; N, 14.06. Found: C, 19.34; H, 5.16; N, 14.31%.

$\{[Zn(tren)]_3(\mu_3\text{-}CO_3)\}(ClO_4)_4\cdot H_2O$ (3). The complex was prepared from $[Zn(tren)(H_2O)](ClO_4)_2$ in the same way as described for **1**. A 63.4% yield of colorless block crystals was obtained, suitable for X-ray analysis. IR cm^{-1} (KBr pellet): 3227s, 2927s, 1597m, 1465s, 1392s, 1364w, 1319m, 1286m, 1133s, 884s, 847m, 741m, 622m. Anal. Calcd for $C_{19}H_{56}N_{12}Cl_4O_{20}Zn_3$: C, 20.55; H, 5.08; N, 15.13. Found: C, 20.88; H, 5.13; N, 15.40%.

$\{[Zn(tren)]_2(\mu\text{-}CO_3H)\}(ClO_4)_3$ (4). The complex was prepared from $[Zn(tren)(H_2O)](ClO_4)_2$ in the same way as described for **2**. A 29.9% yield of colorless cubic crystals was obtained. IR cm^{-1} (KBr pellet): 3219s, 2919m, 1600s, 1464s, 1457m, 1394m, 1365m, 1318s, 1274s, 1077s, 988s, 940m, 883s, 842w, 745m, 636m. Anal. Calcd for $C_{13}H_{39}N_8Cl_3O_{16}Zn_2$: C, 18.66; H, 5.18; N, 13.39. Found: C, 18.52; H, 5.28; N, 13.88%.

$\{[Zn(tren)]_2(\mu\text{-}OH)\}(ClO_4)_3$ (5). The complex was prepared from $[Zn(tren)(H_2O)](ClO_4)_2$ in the same way as described for **4**, but the pH value was adjusted to *ca.* 10.0 when a 45.0% yield of colorless cubic crystals was obtained. IR cm^{-1} (KBr pellet): 3616m, 3299s, 2891s, 1594s, 1476m, 1455m, 1395w, 1366w, 1319s, 1088s, 986s, 886m, 747w, 625s. Anal. Calcd for $C_{12}H_{37}N_8Cl_3O_{13}Zn_2$: C, 19.51; H, 5.05; N, 15.17. Found: C, 19.63; H, 5.25; N, 15.28. The coresponding Cu(II) complex can be isolated in an analogous way.

Potentiometric titration

An automatic titrator (Metrohm 702SM Titrino) coupled to a Metrohm electrode was used and calibrated according to the Gran method.[26] The electrode system was calibrated with buffers and checked by titration of $HClO_4$ with 0.10 M NaOH. All titrations were carried out under Ar atmosphere, at 25.0 ± 0.1 °C and at an ionic strength of 0.25 M using $NaClO_4$, which is known to be a very weak donor. An aqueous solution (20 mL) of the ligand (1.00 mM) with 3 equivalents of $HClO_4$ (3.00 mM) in the absence (for determination of the ligand protonation constant K_n) or in the presence of one equivalent of Cu(II) ions (for determination of the complex-formation constant, K_{ML}, and the deprotonation constant of the coordinated water molecule in the complex, K_a) was titrated with standard 0.1 M NaOH aqueous solution. Duplicate measurements were performed, for which the experimental error was below 1%. The titration data were fitted with the PSEQUAD program to calculate all equilibrium constants.[27] The obtained distribution curve for the various species is shown in Fig. 1.

Spectral measurements

Infrared spectra were recorded on a Nicolet 5SX instrument using KBr pellet method. UV-Vis absorption spectra were recorded on a SHIMADZU UV-2101PC scanning spectrophotometer using a tandem cuvette at 25 °C. The spectra of 2.5 mM $[Cu(tren)(H_2O)](ClO_4)_2$ were recorded in the absence and presence of 0.10 M $NaHCO_3$ as a function of pH, respectively. The obtained spectra and absorbance at 340 nm as a function of pH are shown in Fig. 2. ^{13}C NMR measurements were performed on a Bruker DPX 300 (300 MHz) NMR spectrometer. The spectra of 25 mM $[Zn(tren)(H_2O)](ClO_4)_2$ were recorded in the presence of 75 mM $NaH^{13}CO_3$ as a function of pH in the range 5 to 12. The obtained spectral data are listed in Table 1.

X-Ray structure analysis

Analyses of a blue block single crystal of $\{[Cu(tren)]_3(\mu_3\text{-}CO_3)\}(ClO_4)_4\cdot H_2O$ (**1**) and a colorless block crystal of $\{[Zn(tren)]_3(\mu_3\text{-}CO_3)\}(ClO_4)_4\cdot H_2O$ (**3**) were carried out with a Philips PW1100/10 diffractometer, which uses an equatorial geometry, with graphite monochromated Mo-Kα radiation. Cell parameters for all complexes were determined from automatic centering of 25 reflections in all 8 symmetrical settings

and refined by least-squares refinement. Intensity data were collected using the $\omega/2\theta$-scan technique and corrected for Lorentz and polarization effects.[28] These structures were solved by direct methods using SIR-92 computer program[29a] and refined by full-matrix least-squares methods on F^2 using the SHELXL-93 program.[29b] Hydrogen atoms were located partially from a difference synthesis and refined with an overall isotropic thermal parameter. The remaining H atoms linked to nitrogen were not located.

Crystallographic data and data collection parameters are summarized in Table 2. Selected bond distances and bond angles are given in Tables 3 and 4. Labeled diagrams of complexes **1** and **3** are shown in Figs. 3 and 4, respectively.

CCDC reference numbers 156016 and 156017.

See http://www.rsc.org/suppdata/dt/b1/b100160o/ for crystallographic data in CIF or other electronic format.

Kinetic measurements

The complex solution was prepared freshly with millipore water directly before the kinetic measurements. The HCO_3^- solutions were prepared by dissolving $NaHCO_3$ crystals and 0.2 M $HClO_4$ was added slowly to adjust the pH to the appropriate value and used within 5 h.[11b] Kinetic measurements were performed at 25.0 ± 0.1 °C on a Biologic stopped-flow SFM-3 instrument, and monitored with an on-line data acquisition and handling system. One syringe was filled with the Cu(tren)-$(H_2O)^{2+}$/HCO_3^- solution (pH ≈ 6.1) and the other syringe with buffer solution (Ampso, pH ≈ 9.1). The complex-formation reaction was studied as a function of [Cu(tren)$(H_2O)^{2+}$] and [HCO_3^-], respectively. The ionic strength was adjusted to 0.25 M with $NaClO_4$. The absorbance–time trace was recorded and fitted with a single exponential using the OLIS KINFIT (Bogard, GA, 1992) set of programs. The pH values of all solutions were measured immediately before and after the reaction with a Metrohm 632 pH meter equipped with an Ingold V402-S7/120 electrode.

Results and discussion

Synthesis

In general, most carbonato complexes reported here were synthesized by bubbling CO_2 through the solution or by taking up CO_2 directly from the atmosphere under alkaline conditions. The hydroxo form of metal complexes is active towards CO_2 fixation, similar to that for an OH^- anion. A few hydroxo-bridged metal complexes were also found to be active towards CO_2 uptake.[20] Therefore, {[M(tren)]$_2$(μ-OH)}$(ClO_4)_3$ (M = Cu(II), Zn(II)) were prepared directly and CO_2 was then bubbled into their aqueous solutions, respectively. After evaporation in air, the complexes **1** and **3** were obtained. This result shows that the products are independent of whether HCO_3^- or CO_2 is used as reactant. The process, however, strongly depends on the pH of the solution. When the pH is *ca.* 6.5 or between 7.0 and 9.5, bicarbonato and carbonato complexes can be obtained, respectively. When the pH of the solution is higher than 10, hydroxide can substitute coordinated carbonate to form hydroxo complexes. It is, therefore, in general easier to obtain carbonato than bicarbonato complexes, since the pH of the solution hardly goes below 6.5 *via* the bubbling of CO_2 through the solution, unless extra acid is added and a CO_2 atmosphere is maintained.

Crystals of complexes **2**, **4** and **5** could not be obtained. The structural formulation given in the Experimental section is solely based on chemical analyses and IR data. The IR spectra for the μ-HCO_3^- dimeric complexes **2** and **4** closely resemble those for the corresponding μ_3-CO_3^{2-} trimeric complexes **1** and **3**, respectively, with the difference that the band around 1460 cm^{-1} seems to indicate some asymmetric behavior. In the absence of any further structural information we prefer to visualize **2** and **4** as μ-HCO_3^- dimeric complexes based on the kinetic observations reported below.

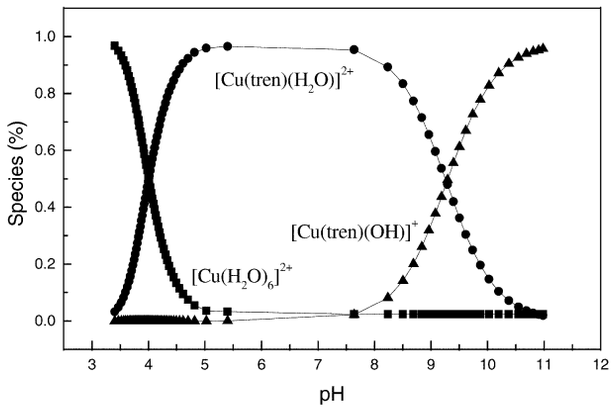

Fig. 1 Concentration distribution for various species as a function of pH for the [Cu(tren)$(H_2O)](ClO_4)_2$ system at 25.0 ± 0.1 °C and ionic strength 0.25 M ($NaClO_4$).

Species distribution

From a fit of the titration data, log K_n (log K_1 = 10.18, log K_2 = 9.52, log K_3 = 8.44), log K_{ML} (18.86 ± 0.04) and pK_a (9.59 ± 0.05) values were obtained. All the results are in good agreement with the literature data.[30] It is seen from Fig. 1 that the formation of [Cu(tren)$(H_2O)]^{2+}$ starts at a pH of *ca.* 4, and this species exists stable in solution as the main species in the pH range 5 to 9. At pH ≈ 7, the coordinated water molecule of [Cu(tren)$(H_2O)]^{2+}$ starts to deprotonate to form [Cu(tren)(OH)]$^+$.

UV-Vis spectra

The obtained UV-Vis spectra in solution are shown in Fig. 2. In the absence of HCO_3^-, the complex [Cu(tren)$(H_2O)]^{2+}$ is characterized by a visible band at 840 nm, which can be assigned to the A′→E″ transition for a five-coordinate D_{3h} Cu(II) complex.[22,31] A new band gradually appeared at 660 nm on increasing the pH. This indicates that the geometry distorts from trigonal bipyramidal to a square pyramidal/octahedral structure due to the formation of [Cu(tren)(OH)]$^+$/{[Cu(tren)]$_2$(μ-OH)}$^{3+}$.[32] A further interesting spectral change occurred in the metal–ligand charge transfer band (340 nm). The absorbance indicates a sigmoidal change in the pH range 9 to 10, which corresponds to a change from [Cu(tren)$(H_2O)]^{2+}$ to [Cu(tren)(OH)]$^+$. The obtained pK_a value (9.7 ± 0.1) is in very good agreement with the pK_a value (9.6) obtained from the titration.

In the presence of HCO_3^-, the absorbance in the range 600–900 nm is similar to, but in the range 300–400 nm (Fig. 2, middle) different from, that in the absence of HCO_3^-. At 340 nm, the absorbance increases from pH 6.0 to reach a maximum at pH *ca.* 10, after which it abruptly decreases with increasing pH to *ca.* 12.5. These changes can be assigned to two processes: firstly, the formation of bicarbonato/carbonato complexes, and secondly, the substitution of coordinated carbonate by OH^-. An apparent pK_a′ (8.2 ± 0.1) is obtained for the equilibrium between bicarbonato and carbonato complexes. When the pH value is less than 6.0, complex species mainly exist in the form of [Cu(tren)$(H_2O)]^{2+}$ due to fast decarboxylation. Therefore, the formation and decomposition of the bicarbonato/carbonato complexes can be detected by a strong absorbance increase at 340 nm in the pH range of 5.5 to 9.5. This wavelength was therefore selected for the kinetic measurements.

^{13}C NMR spectra

Labeled {[Zn(tren)]$_3$(μ_3-$^{13}CO_3$)}$(ClO_4)_4$ revealed a single peak at 168.3 ppm in DMSO-d_6 and at 168.5 ppm in D_2O, respectively, which are in good agreement with that reported for

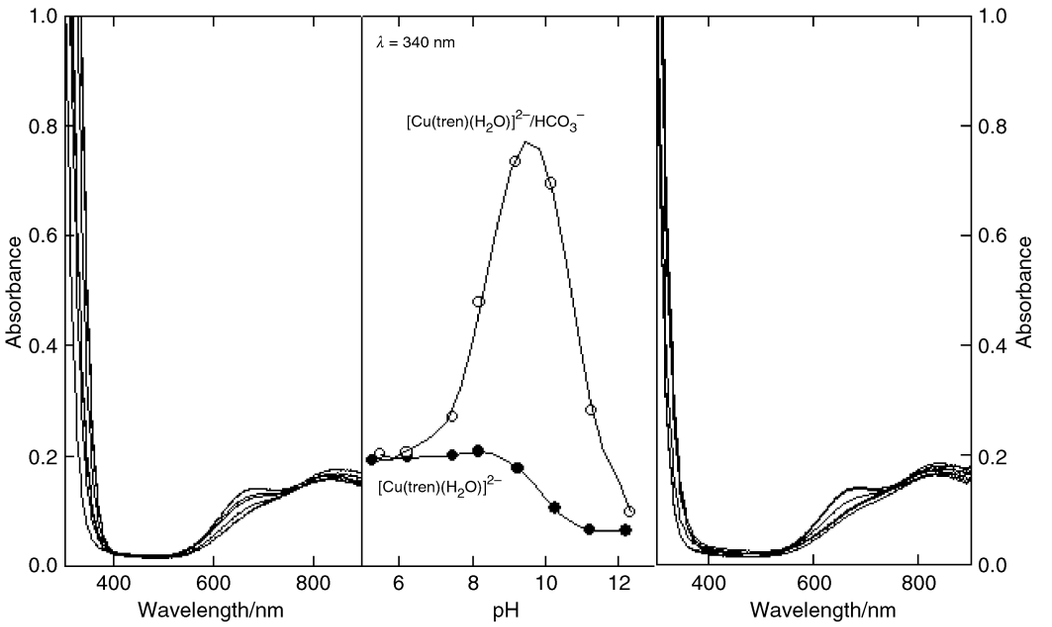

Fig. 2 Visible absorption spectra of 1.25 mM $[Cu(tren)(H_2O)](ClO_4)_2$ (right) and 1.25 mM $[Cu(tren)(H_2O)](ClO_4)_2$/0.10 M $NaHCO_3$ (left) as a function of pH, and of both at 340 nm (middle) at 25.0 ± 0.1 °C and ionic strength 0.25 M ($NaClO_4$).

Table 1 ^{13}C NMR spectral data (δ) for $[Zn(tren)(H_2O)](ClO_4)_2$ in the presence of $NaH^{13}CO_3$ as a function of pH

Ph	CO_2	HCO_3^-	CO_3^{2-}	$\{[Zn(tren)]_x(\mu_x\text{-}OCO_2)\}^{(2x-2)+}$
5.39	127.5	163.1		
5.94	127.5	163.1		
6.46	127.5	163.1		
7.28	127.5	163.1		167.0
8.19	127.0	163.7		167.1
9.25		165.4		167.5/167.7
10.51			169.7/167.5	
11.36			170.8	
12.57			170.8	

other Zn–CO_3 complexes with square pyramidal structure.[11a,33] Furthermore, ^{13}C NMR spectra of $[Zn(tren)(H_2O)]^{2+}$ in the presence of $H^{13}CO_3^-$ in D_2O was studied as a function of pH, and the data are listed in Table 1. At low pH, free $^{13}CO_2$ at 127.5 ppm and $H^{13}CO_3^-$ at 163.1 ppm were observed, whereas at high pH, a peak at 170.8 ppm was observed for free $^{13}CO_3^{2-}$. In the pH range 8 to 11, two peaks were recorded: one is strong and another multiple peak is very weak. The intensity of the weak multiple peak at 167.5–167.7 ppm is only *ca.* 2–3% of the strong one. The strong single peak is assigned to the average value of the chemical shift of free $H^{13}CO_3^-/^{13}CO_3^{2-}$ as a result of fast chemical exchange.[34] The weak multiple peak is assigned to the carbonato complexes formed with increasing pH. This indicates that the species mainly exist in the form of $[Zn(tren)(H_2O)]^{2+}$ in solution in the pH range 6 to 10 even though a large excess of HCO_3^- is present in solution. It is reasonable to expect that $[Cu(tren)(H_2O)]^{2+}$ will exhibit a very similar behavior in solution in the presence of HCO_3^-.

Structures

The structures of two trinuclear carbonato complexes could be resolved. Both complexes crystallize in C-centered monoclinic symmetry (Table 2). The structures were also refined in the triclinic space group type *P*1 with 2 independent crystallographic units ($Z = 2$). This was done since the metrical reduction from the triclinic to the monoclinic unit base with doubled volume matches quite well, but the intensities of the symmetrical equivalent reflections do not. The refinement in both space groups resulted in similar *R* and *S* values. The poor quality of the crystals and the possibly imperfect absorption correction hindered a distinction between *P*1 and *Cc* symmetry. The more common *Cc* assignment was therefore selected for publication purposes.

Table 2 Crystallographic details for $\{[Cu(tren)]_3(\mu_3\text{-}CO_3)\}(ClO_4)_4\cdot H_2O$ (**1**) and $\{[Zn(tren)]_3(\mu_3\text{-}CO_3)\}(ClO_4)_4\cdot H_2O$ (**3**)

	1	**3**
Empirical formula	$C_{19}H_{56}N_{12}Cl_4O_{20}Cu_3$	$C_{19}H_{56}N_{12}Cl_4O_{20}Zn_3$
Formula weight	1105.16	1110.67
T/K	293	293
Wavelength/Å	0.71069	0.71069
Space group	*Cc*	*Cc*
a/Å	13.389(7)	13.371(6)
b/Å	29.290(8)	29.728(6)
c/Å	12.589(6)	12.699(5)
α/°	90	90
β/°	118.82(5)	118.90(2)
γ/°	90	90
V/Å^3	4325(5)	4419(5)
Z	4	4
ρ(calcd)/g cm^{-3}	1.66	1.64
μ/mm^{-1}	1.790	1.940
F(000)	2196	2208
Crystal size/mm	0.65 × 0.38 × 0.45	0.48 × 0.25 × 0.38
Reflections collected	14285	11604
R_1 [$I > 2\sigma(I)$]	0.094	0.061

$\{[Cu(tren)]_3(\mu_3\text{-}CO_3)\}(ClO_4)_4\cdot H_2O$ (1). The μ_3-bridged carbonato complex possesses a pseudo-3-fold molecular symmetry. Each of the three Cu(II) atoms is five-coordinate with the four nitrogen atoms of the tren ligand and one oxygen of the carbonate ligand (Fig. 3, Table 3). The coordination polyhedron of the copper atoms can be described as almost trigonal bipyramidal, although the copper ions are slightly out of the plane of the three primary amine groups by ±0.15 Å. The carbonate group is planar and the three copper ions deviate from this plane by ±0.05 Å. The Cu–O bond lengths in the complex are typical for five-coordinate metal complexes. The CO_3^{2-} group coordinates to the copper ions along the axis of the trigonal bipyramidal structure. This differs from other cases in which the CO_3^{2-} group coordinates to copper ions along the basal plane of the square pyramidal structure.[14,35,36]

Table 3 Selected bond lengths (Å) and angles (°) for {[Cu(tren)]$_3$-(μ_3-CO_3)}$(ClO_4)_4$·H_2O (**1**)

C(1)–O(3)	1.254(13)	C(1)–O(1)	1.295(10)
C(1)–O(2)	1.299(13)	O(1)–Cu(1)	1.922(8)
O(2)–Cu(2)	1.922(9)	O(3)–Cu(3)	1.933(6)
Cu(1)–N(4)	2.041(10)	Cu(1)–N(1)	2.064(9)
Cu(1)–N(3)	2.075(11)	Cu(1)–N(2)	2.071(11)
Cu(2)–N(8)	2.048(11)	Cu(2)–N(6)	2.066(9)
Cu(2)–N(5)	2.047(9)	Cu(2)–N(7)	2.177(10)
Cu(3)–N(12)	2.053(8)	Cu(3)–N(10)	2.091(9)
Cu(3)–N(11)	2.131(12)	Cu(3)–N(9)	2.062(11)
O(3)–C(1)–O(1)	120.3(9)	O(3)–C(1)–O(2)	120.6(7)
O(1)–C(1)–O(2)	119.1(10)	C(1)–O(1)–Cu(1)	121.4(8)
C(1)–O(2)–Cu(2)	119.0(6)	C(1)–O(3)–Cu(3)	119.9(6)
O(1)–Cu(1)–N(4)	173.4(4)	O(1)–Cu(1)–N(1)	94.4(4)
O(1)–Cu(1)–N(2)	90.7(4)	O(1)–Cu(1)–N(3)	102.3(3)
O(2)–Cu(2)–N(8)	179.0(4)	O(2)–Cu(2)–N(6)	94.4(4)
O(2)–Cu(2)–N(7)	97.9(4)	O(2)–Cu(2)–N(5)	94.0(4)
O(3)–Cu(3)–N(12)	178.1(4)	O(3)–Cu(3)–N(10)	94.5(3)
O(3)–Cu(3)–N(9)	96.7(3)	O(3)–Cu(3)–N(11)	94.4(3)

Table 4 Selected bond lengths (Å) and angles (°) for {[Zn(tren)]$_3$-(μ_3-CO_3)}$(ClO_4)_4$·H_2O (**3**)

C(1)–O(3)	1.252(11)	C(1)–O(1)	1.278(12)
C(1)–O(2)	1.300(10)	O(1)–Zn(1)	1.998(6)
O(2)–Zn(2)	2.007(7)	O(3)–Zn(3)	1.998(7)
Zn(1)–N(4)	2.268(8)	Zn(1)–N(1)	2.084(9)
Zn(1)–N(3)	2.084(9)	Zn(1)–N(2)	2.077(9)
Zn(2)–N(8)	2.296(10)	Zn(2)–N(6)	2.058(9)
Zn(2)–N(5)	2.035(12)	Zn(2)–N(7)	2.072(9)
Zn(3)–N(12)	2.265(12)	Zn(3)–N(10)	2.122(9)
Zn(3)–N(11)	2.086(9)	Zn(3)–N(9)	2.057(10)
O(3)–C(1)–O(1)	121.3(7)	O(3)–C(1)–O(2)	119.9(9)
O(1)–C(1)–O(2)	118.8(8)	C(1)–O(1)–Zn(1)	113.9(5)
C(1)–O(2)–Zn(2)	114.8(6)	C(1)–O(3)–Zn(3)	116.0(6)
O(1)–Zn(1)–N(4)	178.4(3)	O(1)–Zn(1)–N(1)	96.8(3)
O(1)–Zn(1)–N(2)	101.3(3)	O(1)–Zn(1)–N(3)	98.5(3)
O(2)–Zn(2)–N(8)	170.9(3)	O(2)–Zn(2)–N(6)	97.2(3)
O(2)–Zn(2)–N(7)	93.9(3)	O(2)–Zn(2)–N(5)	108.0(3)
O(3)–Zn(3)–N(12)	173.8(3)	O(3)–Zn(3)–N(10)	96.0(4)
O(3)–Zn(3)–N(9)	104.7(3)	O(3)–Zn(3)–N(11)	97.1(4)

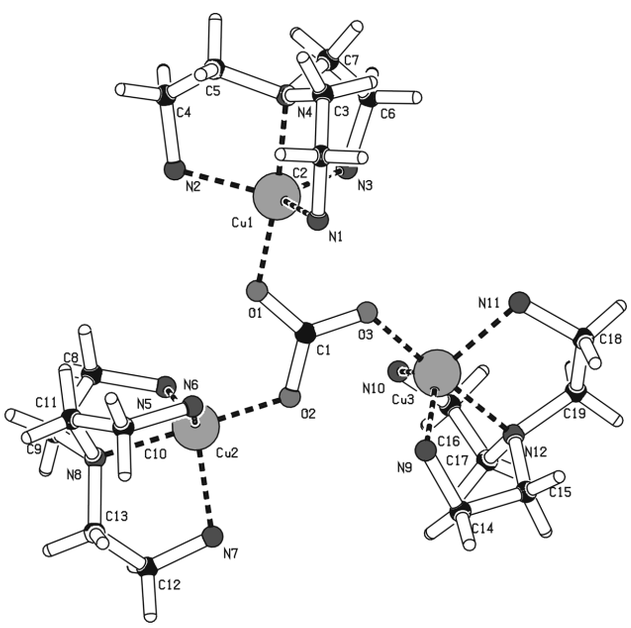

Fig. 3 Molecular structure of {[Cu(tren)]$_3$(μ_3-CO_3)}$^{4+}$.

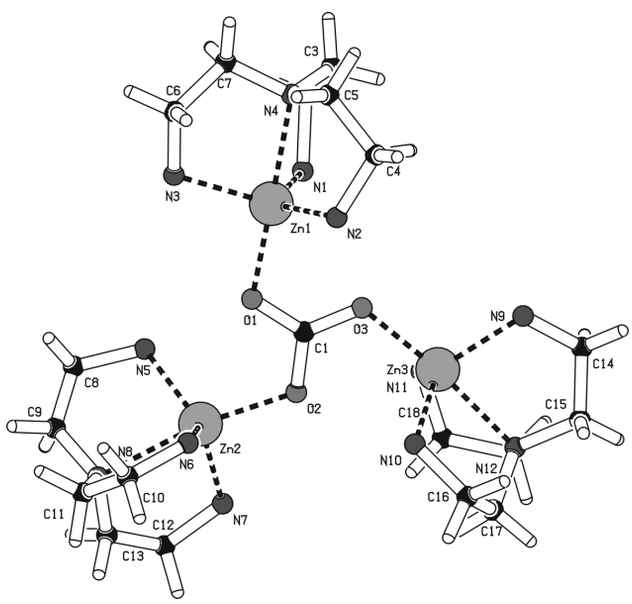

Fig. 4 Molecular structure of {[Zn(tren)]$_3$(μ_3-CO_3)}$^{4+}$.

{[Zn(tren)]$_3$(μ_3-CO_3)}$(ClO_4)_4$·H_2O (3). This structure is very similar to that of complex **1**. The μ_3-bridged carbonato complex possesses a pseudo-3-fold molecular symmetry. Each of the three zinc atoms is five-coordinate with the four nitrogen atoms of the tren ligand and one oxygen of the carbonate ligand (Fig. 4, Table 4). The coordination polyhedron of the zinc atoms can be described as almost trigonal bipyramidal, although the zinc ions are slightly out of the plane of the three primary amine groups by ±0.06 Å. The carbonate group is planar and the three zinc atoms deviate from this plane by ±0.05 Å. The Zn–O bond lengths in complex **3** are slightly longer than the Cu–O bond lengths in complex **1**. The structural characteristics are very similar to those for other zinc complexes[20] and differ only slightly from others.[11a,12,14,36c] The structures of the reported μ_3-carbonate bridged trinuclear complexes are summarized in Table 5. Tripodal ligands such as tren and tmpa clearly favor a trigonal bipyramidal structure, whereas cyclic N_4 chelates such as cyclen favor a tetragonal pyramidal structure around the metal centers.

Kinetics

The kinetics of the reaction of $[Cu(tren)(H_2O)]^{2+}$ with HCO_3^- was studied in detail using stopped-flow and T-jump techniques. On mixing two syringes filled with a HCO_3^- solution and a mixture of $[Cu(tren)(H_2O)]^{2+}$/buffer, respectively, in the stopped-flow instrument, no kinetic trace could be observed in the pH range 6 to 9, although a significant spectral change did occur on mixing, as was shown using a tandem cuvette. Furthermore, the reaction could also not be observed using the T-jump technique. In view of the relatively high pK_a value (9.59) of $[Cu(tren)(H_2O)]^{2+}$ and the low pK_{a1} value (6.35) of HCO_3^-, the reaction between $[Cu(tren)(OH)]^+$ and CO_2 may not be important in the selected pH range. The results, therefore, indicate that substitution of coordinated H_2O by HCO_3^- in $[Cu(tren)(H_2O)]^{2+}$ must be very fast, which is quite different from that observed for other metal complexes studied before.[1i]

A clear kinetic trace could only be observed on the stopped-flow instrument when the two syringes were filled with a mixture of $[Cu(tren)(H_2O)]^{2+}$/HCO_3^- and a buffer solution, respectively (see Experimental section), whereby a pH jump from 6 to 9 could be induced. The resulting trace exhibited good first-order behavior, and k_{obs} was measured as a function of $[Cu(tren)(H_2O)^{2+}]$ and $[HCO_3^-]$, respectively, for which the results are shown in Fig. 5. Very surprising is our observation that k_{obs} is independent of $[HCO_3^-]$, but depends linearly on $[Cu(tren)(H_2O)^{2+}]$, although an excess of HCO_3^- was employed under all conditions. This is an unusual observation for pseudo-first-order kinetics, and in fact the opposite concentration dependencies were expected. This means that all reactions

Table 5 Summary of reported μ_3-CO_3^{2-} complexes

Complex	Closed metal geometry	CO_3^{2-} position	Ref.
$\{[Cu(pip)(H_2O)]_3(\mu_3\text{-}CO_3)\}(ClO_4)_4$	TP	Basal plane	35
$\{[Zn(dpt)]_3(\mu_3\text{-}CO_3)\}(ClO_4)_4$	Tetrahedral	Apical	12
$\{[Cu(medpt)]_3(\mu_3\text{-}CO_3)\}(ClO_4)_4$	TP	Basal plane	36(*a*)
$\{[Ni(medpt)]_3(\mu_3\text{-}CO_3)(NCS)_4\}$	Octahedral	Apical	36(*b*)
$\{[Zn_3(bpy)_6(\mu_3\text{-}CO_3)(H_2O)_2\}(ClO_4)_4$	Octahedral and TBP	Apical and equatorial plane	36(*c*)
$\{[Cu_6(bpy)_{10}(\mu_3\text{-}CO_3)_2(\mu_2\text{-}OH)_2]\}(ClO_4)_6$	TP	Basal plane and axial position	36(*d*)
$\{[Zn(cyclen)]_3(\mu_3\text{-}CO_3)\}(ClO_4)_4$	TP	Apical	11(*a*)
$\{[Cu([15]aneN_3O_2)]_3(\mu_3\text{-}CO_3)\}(ClO_4)_4$	TP	Basal plane	14
$\{[Zn([15]aneN_3O_2)]_3(\mu_3\text{-}CO_3)\}(ClO_4)_4$	TBP	Equatorial plane	14
$\{[Zn(tmpa)]_3(\mu_3\text{-}CO_3)\}(ClO_4)_4$	TBP	Apical	29
$\{[Cu(tren)]_3(\mu_3\text{-}CO_3)\}(ClO_4)_4$	TBP	Apical	This work
$\{[Zn(tren)]_3(\mu_3\text{-}CO_3)\}(ClO_4)_4$	TBP	Apical	This work

TP = tetragonal pyramidal, TBP = trigonal bipyramidal. pip = 2-[2-(2-pyridy)ethyliminoethyl]pyridine, dpt = bis(3-aminopropyl)amine, medpt = bis(3-aminopropyl)methylamine, cyclen = tetraazacyclododecane, [15]aneN$_3$O$_2$ = 1,4-dioxa-7,10,13-triazacyclopentadecane, bpy = 2,2′-bipyridine, tmpa = tris(2-pyridyl)methylamine, tren = tris(2-aminoethyl)amine.

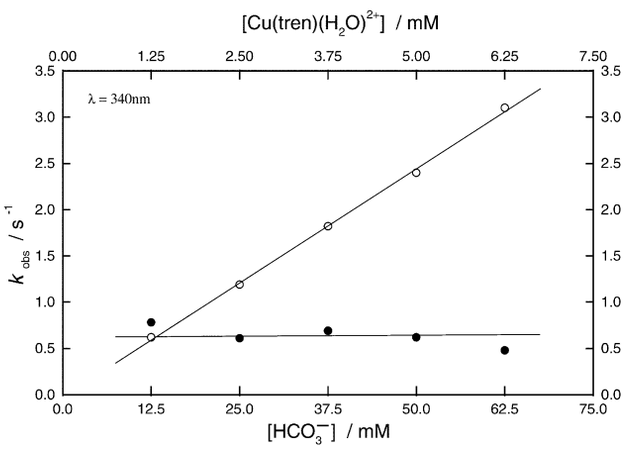

Fig. 5 Plot of k_{obs} *versus* [Cu(tren)$(H_2O)^{2+}$] (○) at 50 mM HCO_3^-, and plot of k_{obs} *versus* [HCO_3^-] (●) at 1.25 mM Cu(tren). Temperature = 25.0 ± 0.1 °C and ionic strength = 0.25 M ($NaClO_4$).

involving HCO_3^- must be non-rate-determining steps, and a possible explanation is that the pH-jump introduces a relaxation process.

In the light of the high lability of coordinated H_2O in [Cu(tren)$(H_2O)]^{2+}$,[22] substitution by HCO_3^- in eqn. (2) is expected to be a rapid equilibration. In general, monomeric bicarbonato complexes are unstable, especially in the case of a monodentate structure and undergo reverse aquation or decarboxylation. It is therefore reasonable to suggest that during the reaction of $[Cu(tren)(H_2O)]^{2+}$ with HCO_3^-, the unstable monodentate $[Cu(tren)OCO_2H]^+$ complex will only be formed at low concentrations, *i.e.* an unfavorable equilibrium position will exist at low pH. The observed kinetics induced by pH-jump could therefore correspond to the reaction of the intermediate bicarbonate complex with the remaining $[Cu(tren)(H_2O)]^{2+}$ in solution in order to account for the observed dependence on the concentration of $[Cu(tren)(H_2O)]^{2+}$. We suggest that the subsequent reaction involves the binding of the uncoordinated carboxylate oxygen to another copper ion in an intermolecular way to form a binuclear carbonato complex as shown in reactions (2) to (4). Equilibria (2) and (3) are established rapidly

$$[Cu(tren)(H_2O)]^{2+} + HCO_3^- \rightleftharpoons [Cu(tren)OCO_2H]^+ + H_2O \quad \text{fast} \quad (2)$$

$$[Cu(tren)OCO_2H]^+ \rightleftharpoons [Cu(tren)OCO_2] + H^+ \quad \text{fast} \quad (3)$$

$$[Cu(tren)OCO_2] + [Cu(tren)(H_2O)]^{2+} \rightleftharpoons \{[Cu(tren)]_2O_2CO\}^{2+} + H_2O \quad \text{slow} \quad (4)$$

and mainly account for the equilibrium situation at pH 6. On mixing this solution with a buffer of pH 9 in the stopped-flow instrument, a rapid deprotonation of coordinated bicarbonate occurs as shown in reaction (3) and the system relaxes to a new equilibrium situation which now involves the rate-determining formation of the dimeric species.

In terms of the suggested relaxation kinetics induced by the pH-jump, the rate expression for the rate-determining step is given by eqn. (5) under the condition that the observed

$$k_{obs} = 1/\tau = k_4\{[Cu(tren)OCO_2]_e + [Cu(tren)(H_2O)^{2+}]_e\} + k_{-4} \quad (5)$$

relaxation process involves relatively small concentration changes.[37] This seems to be valid since the ^{13}C-NMR spectra recorded for the corresponding Zn(II) complexes, indicated that only low concentrations of the carbonato complexes exist in solution, even in the presence of a large excess of bicarbonate and at higher pH. Since equilibrium (2) is unfavorable, *i.e.* $[Cu(tren)(H_2O)^{2+}] \gg [Cu(tren)OCO_2]$ as pointed out above, the rate equation simplifies as shown in eqn. (6), which can then

$$k_{obs} = 1/\tau = k_4[Cu(tren)(H_2O)^{2+}] + k_{-4} \quad (6)$$

account for the independence of the observed rate constant on the bicarbonate concentration and the linear dependence on the $[Cu(tren)(H_2O)]^{2+}$ concentration (see Fig. 5).

The second order rate constant of 494 ± 10 M^{-1} s^{-1}, calculated from the slope of the plot in Fig. 5, represents the rate constant for the formation of the carbonate bridged complex, *i.e.* k_4. The observed kinetics will be almost independent of the bicarbonate concentration, since this will only control the extent to which the $[Cu(tren)OCO_2H]^+$ complex is formed during the rapid equilibration of the aqua complex with bicarbonate. In fact, the data in Fig. 5 show a slight decrease in rate constant with increasing bicarbonate concentration at a fixed $[Cu(tren)(H_2O)]^{2+}$ concentration. This is in line with the suggested reaction mechanism, since on increasing the bicarbonate concentration, less aqua complex will be available for the subsequent formation of the bridged complex and k_{obs} will decrease according to eqn. (6). Ultimately, this interpretation is only valid under the conditions that equilibrium (2) is unfavorable such that only a low concentration of the bicarbonato complex exists in solution prior to the pH-jump. This is in line with the spectral observations reported in Fig. 2 and the ^{13}C-NMR spectra reported for the corresponding Zn(II) complex.

The UV-Vis spectral study shows that the coordination geometry of the copper ion in $[Cu(tren)(H_2O)]^{2+}$ adopts a distorted trigonal bipyramidal structure, but not an octahedral one in solution in the presence of HCO_3^-, even if OH^- acts as a

nucleophile at high pH. In view of these properties of [Cu(tren)$(H_2O)]^{2+}$, the ring-closed bicarbonato complex is hardly formed and therefore, the unstable monomeric bicarbonato complex coordinates to another $[Cu(tren)(H_2O)]^{2+}$ ion. The structures of two binuclear bicarbonato copper and zinc complexes with macrocyclic ligands were previously reported.[38,39] In our case, chemical characterization showed that analogous complexes were obtained at low pH, but X-ray structure analysis failed. We were, however, recently successful in isolating two monomeric bicarbonato complexes of bis(phenanthroline)copper(II), *viz*. $[Cu(phen)_2O_2COH]ClO_4$ and $[Cu(phen)_2OCO_2H]ClO_4$, in which bicarbonate is coordinated as a bidentate and monodentate ligand, respectively.[40]

Although HCO_3^- was used in a large excess in the kinetic study, ^{13}C NMR spectra of $[Zn(tren)(H_2O)]^{2+}/H^{13}CO_3^-$ showed that the concentration of intermediate and product complexes is very low in solution. The structural characterization of the isolated products at pH 9 showed that the carbonato-bridged trinuclear metal complex was obtained as shown in reaction (7).

$$[Cu(tren)]_2O_2CO^{2+} + [Cu(tren)(H_2O)]^{2+} \longrightarrow [Cu(tren)]_3(\mu_3\text{-}CO_3)^{4+} + H_2O \quad (7)$$

An overall possible mechanism for carbonation is proposed in Scheme 2.

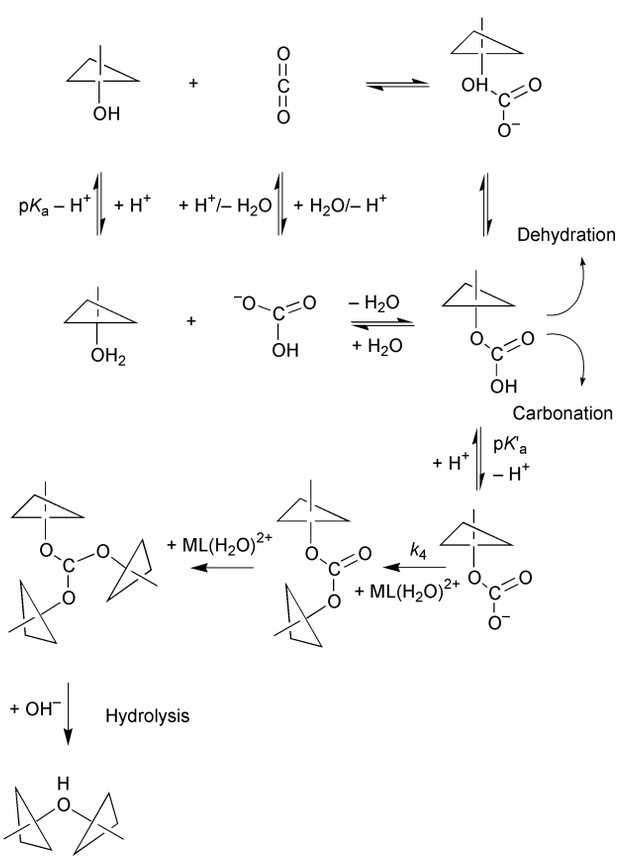

Scheme 2 Proposed mechanism for carbonation of CuN_4 with an axial water molecule in the trigonal bipyramidal structure.

The substitution of H_2O in $[Cu(tren)(H_2O)]^{2+}$ by HCO_3^- is a rapid process, but produces only low concentrations of the monomeric bicarbonato species at low pH. With increasing pH, carbonation is enhanced, so that the unstable monodentate bicarbonato intermediate deprotonates and reacts with the excess $[Cu(tren)(H_2O)]^{2+}$ to form a stable binuclear carbonato complex, though only present in solution at low concentrations. Subsequently, the binuclear carbonato complex produces the more stable $\{[Cu(tren)]_3(\mu_3\text{-}CO_3)\}^{4+}$ ion in (7), which could be isolated and characterized as perchlorate salt. The CO_2 uptake reaction route does not compete efficiently presumably due to the high pK_a value of $[Cu(tren)(H_2O)]^{2+}$, *i.e*. the low fraction of hydroxo complex present in solution.

Carbonation *vs.* hydration. The obtained rate constant for the formation of the binuclear bicarbonato Cu(II) complex lies within the range of values reported for the hydration reaction of other model complexes.[4,6,8c,11,19] All the results indicate that the $[Zn(tren)(H_2O)]^{2+}$ complex behaves similarly in solution to the $[Cu(tren)(H_2O)]^{2+}$ complex, although the Zn(II) ion is spectroscopically inactive and kinetic measurements on the formation of the binuclear carbonato Zn(II) complex could not be performed. In our earlier work on the hydration mechanism of CO_2,[11b,c] the apparent catalytic rate constant $(k^h_{cat})_{obs}$ for the tetragonal pyramidal $[Zn([12]aneN_4)(H_2O)]^{2+}$ complex ([12]aneN$_4$ = tetraazacyclododecane) was found to be much higher than for the tetrahedral $[Zn([12]aneN_3)(H_2O)]^{2+}$ ([12]aneN$_3$ = triazacyclododecane) complex ion, and is the highest of all model complexes studied up to now. However, a comparison with the structure of the enzyme indicates that the structure of the latter complex is much closer to the active site of the enzyme than in the case of the former complex.[7,11] In the case of $[Zn([12]aneN_4)(H_2O)]^{2+}$, the tetragonal pyramidal structure will cause the unstable monodentate bicarbonate intermediate to form a polynuclear complex. However, for $[Zn([12]aneN_3)(H_2O)]^{2+}$ the tetrahedral geometry can provide a fifth coordination site for the monodentate bicarbonate intermediate to advance to the bidentate carbonate complex, thus favoring the carbonation process.

Conclusions

The kinetic study of the reaction of $[Cu(tren)(H_2O)]^{2+}$ with HCO_3^- indicates that the five-coordinate copper complex with trigonal bipyramidal structure is active towards substitution of H_2O by HCO_3^- when H_2O is located in the axial position. The complex-formation reaction is so fast that it could not be studied by stopped-flow and T-jump techniques. The unstable monodentate bicarbonato intermediate produces on deprotonation the binuclear carbonato complex in a kinetically observed step. CO_2 uptake by the investigated $[Cu(tren)(H_2O)]^{2+}$ complex is prevented by the relatively high pK_a value of the aqua complex, which results in the formation of $[Cu(tren)OH]^+$ in a pH range where too little CO_2 is present in solution. Thus the contribution of the carbonation process to the overall observed reaction should also be considered in studies on model complexes.

Acknowledgments

The authors gratefully acknowledge financial support from the Deutsche Forschungsgemeinschaft and Fonds der Chemischen Industrie, as well as a fellowship to Z.-W. M from the Alexander von Humboldt Foundation. We thank Dr F. Thaler and Dr A. Zahl (University of Erlangen-Nürnberg) for their kind assistance with the titration and NMR measurements.

References

1 CA and its models have been extensively reviewed: (*a*) E. Kimura, K. Koike and M. Shionoya, *Struct. Bonding* (*Berlin*), 1997, **89**, 1; (*b*) W. N. Lipscomb and N. Strater, *Chem. Rev.*, 1996, **96**, 2375; (*c*) E. Kimura, *Prog. Inorg. Chem.*, 1994, **11**, 443; (*d*) S. J. Dodgson, R. E. Tashian, G. Gros and N. D. Carter, *The Carbonic Anhydrases*, Plenum Press, New York, 1991; (*e*) D. W. Christianson, *Adv. Protein Chem.*, 1991, **41**, 281; (*f*) F. Botre, G. Gros and B. T. Storey, *Carbonic Anhydrase*, VCH, Weinheim, Germany, 1991; (*g*) D. N. Silverman and S. Lindskog, *Acc. Chem. Res.*, 1988, **21**, 30; (*h*) J. E. Coleman, in *Zinc Enzymes*, ed. I. Bertini, C. Luchinat, W. Maret and M. Zeppezauer, Birkhäuser, Boston, 1986, p. 317; (*i*) D. A. Palmer and R. van Eldik, *Chem. Rev.*, 1983, **83**, 51; (*j*) I. Bertini,

C. Luchinat and A. Scozzafava, *Struct. Bonding* (*Berlin*), 1982, **48**, 45.
2 (a) H. Steiner, B.-H. Jonsson and S. Lindskog, *Eur. J. Biochem.*, 1975, **59**, 253; (*b*) R. S. Rowlett and D. N. Silverman, *J. Am. Chem. Soc.*, 1982, **104**, 6737; (*c*) M. Hartmann, T. Clark and R. van Eldik, *J. Am. Chem. Soc.*, 1997, **119**, 7843; (*d*) K. M. Merz and L. Banci, *J. Am. Chem. Soc.*, 1997, **119**, 863; (*e*) Y.-J. Zheng and K. M. Merz, *J. Am. Chem. Soc.*, 1992, **114**, 10498; (*f*) D. R. Garmer and M. Krauss, *J. Am. Chem. Soc.*, 1992, **114**, 6487; (*g*) K. M. Merz, R. Hoffmann and M. J. S. Dewar, *J. Am. Chem. Soc.*, 1989, **111**, 5636.
3 (*a*) Y. Xue, J. Vidgren, L. A. Svensson, A. Liljas, B.-H. Jonsson and S. Lindskog, *Proteins*, 1993, **15**, 80; (*b*) K. Hakansson, M. Carlsson, A. Svensson and A. Liljas, *J. Mol. Biol.*, 1992, **227**, 1192; (*c*) S. K. Nair and D. Christianson, *J. Am. Chem. Soc.*, 1991, **113**, 9455.
4 P. Woolley, *Nature* (*London*), 1975, **258**, 677.
5 M. L. M. Pennings, D. N. Reinhoudt, S. Harkema and G. J. van Hummel, *J. Am. Chem. Soc.*, 1980, **102**, 7571.
6 (*a*) R. S. Brown, N. J. Curtis and J. Huguet, *J. Am. Chem. Soc.*, 1981, **103**, 6953; (*b*) R. S. Brown, D. Salmon, N. J. Curtis and S. Kusuma, *J. Am. Chem. Soc.*, 1982, **104**, 3188; (*c*) H. Slebocka-Tilk, J. L. Cocho, Z. Frakman and R. S. Brown, *J. Am. Chem. Soc.*, 1984, **106**, 2421.
7 (*a*) T. Koike, M. Takamura and E. Kimura, *J. Am. Chem. Soc.*, 1994, **116**, 8443; (*b*) T. Koike and E. Kimura, *J. Am. Chem. Soc.*, 1991, **113**, 8935; (*c*) E. Kimura, T. Shiota, T. Koike, M. Shiro and M. Kodama, *J. Am. Chem. Soc.*, 1990, **112**, 5805.
8 (*a*) M. Kimblin, W. E. Allen and G. Parkin, *J. Chem. Soc.*, *Chem. Commun.*, 1995, 1813; (*b*) A. Looney and G. Parkin, *Inorg. Chem.*, 1994, **33**, 1234; (*c*) A. Looney, R. Han, K. McNeill and G. Parkin, *J. Am. Chem. Soc.*, 1993, **115**, 4690.
9 (*a*) R. Alsfasser, M. Ruf, S. Trofimenko and H. Vahrenkamp, *Chem. Ber.*, 1993, **126**, 685; (*b*) R. Alsfasser, S. Trofimenko, A. Looney, G. Parkin and H. Vahrenkamp, *Inorg. Chem.*, 1991, **30**, 4098.
10 N. Kitajima, S. Hikichi, M. Tanaka and Y. Moro-oka, *J. Am. Chem. Soc.*, 1993, **115**, 5496.
11 (*a*) A. Schrodt, A. Neubrand and R. van Eldik, *Inorg. Chem.*, 1997, **36**, 4579; (*b*) X. Zhang and R. van Eldik, *Inorg. Chem.*, 1995, **34**, 5606; (*c*) X. Zhang, R. van Eldik, T. Koike and E. Kimura, *Inorg. Chem.*, 1993, **32**, 5749.
12 T. Itoh, Y. Fujii, T. Tada, Y. Yoshikawa and H. Hisada, *Bull. Chem. Soc. Jpn.*, 1996, **69**, 1265.
13 L. Cronin, B. Greener, S. P. Foxon, S. L. Heath and P. H. Walton, *Inorg. Chem.*, 1997, **36**, 2594.
14 C. Bazzicalupi, A. Bencini, A. Bianchi, F. Corana, V. Fusi, P. Giorgi, P. Paoli, P. Paoletti, B. Valtancoli and C. Zanchini, *Inorg. Chem.*, 1996, **35**, 5540.
15 R. W. Hay, A. K. Basak and M. P. Pujari, *J. Chem. Soc.*, *Dalton Trans.*, 1989, 197.
16 J. Chin and V. Jubian, *J. Chem. Soc.*, *Chem. Commun.*, 1989, 839.
17 (*a*) P. R. Norman, A. Tate and R. Rich, *Inorg. Chim. Acta*, 1988, **145**, 211; (*b*) P. R. Norman, *Inorg. Chim. Acta*, 1987, **130**, 1.
18 S. H. Gellman, R. Petter and R. Breslow, *J. Am. Chem. Soc.*, 1986, **108**, 2388.
19 L. M. P. Marcel and N. R. David, *J. Am. Chem. Soc.*, 1980, **102**, 7571.
20 N. N. Murthy and K. D. Karlin, *J. Chem. Soc.*, *Chem. Commun.*, 1993, 1236.
21 S. Lindskog and P. O. Nyman, *Biochim. Biophys. Acta*, 1964, **85**, 462.
22 (*a*) D. H. Powell, A. E. Merbach, I. Fabian, S. Schindler and R. van Eldik, *Inorg. Chem.*, 1994, **33**, 4468; (*b*) A. M. Dittler-Kingemann, C. Orvig, F. E. Hahn, F. Thaler, C. D. Hubbard, R. van Eldik, S. Schindler and I. Fabian, *Inorg. Chem.*, 1996, **35**, 7798.
23 Y. Xue, J. Vidgren, L. A. Svensson, A. Liljas, B.-H. Jonsson and S. Lindskog, *Proteins*, 1993, **15**, 80.
24 V. Kumar and K. K. Kannan, *J. Mol. Biol.*, 1994, **241**, 226.
25 L. V. Interrante, *Inorg. Chem.*, 1968, **7**, 943.
26 G. Gran, *Acta Chem. Scand.*, 1950, **4**, 559.
27 J. L. David, *Computational Methods for the Determination of Formation Constants*, Plenum Press, New York, 1985, ch. 8.
28 (*a*) M. Gomm, PWCOM-6.6, Single-crystal Diffractometry-hardware and software, Crystallographic Computing 6, IUCr, Oxford University Press, Oxford, 1993; (*b*) G. Liehr, Inread, Datenreduktion am PW1100, University of Erlangen-Nürnberg, Germany, 1981.
29 (*a*) A. Altomare, G. Cascarano, C. Giacovazzo, A. Guagliardi, M. C. Burla, G. Polidori and M. Camalli, SIR-92, A Package for Solving Crystal Structures by Direct Methods, *J. Appl. Crystallogr.*, 1992, **22**, 389; (*b*) G. M. Sheldrick, SHELXL-93, A System for Crystal Structure Refinement, University of Göttingen, Germany, 1993.
30 (*a*) G. Anderegg and V. Gramlich, *Helv. Chim. Acta*, 1994, **77**, 685; (*b*) R. M. Smith and A. E. Martell, *Critical Stability Constants*, Plenum Press, New York, 1989, vol. 6, 2nd suppl., pp. 210–211.
31 F. Thaler, C. D. Hubbard, F. W. Heinemann, R. van Eldik, S. Schindler, I. Fabian, A. M. Dittler-Kingemann, F. E. Hahn and C. Orvig, *Inorg. Chem.*, 1998, **37**, 4022.
32 B. J. Hathway, *J. Chem. Soc.*, *Dalton Trans.*, 1972, 1196.
33 M. Kato and T. Ito, *Inorg. Chem.*, 1985, **24**, 504.
34 E. T. Strom and D. E. Woessner, *J. Am. Chem. Soc.*, 1981, **103**, 1255.
35 G. Kolks, S. J. Lippard and J. V. Waszczak, *J. Am. Chem. Soc.*, 1980, **102**, 4832.
36 (*a*) A. Escuer, R. Vicente, E. Penallba, X. Solans and M. Font-Bardia, *Inorg. Chem.*, 1996, **35**, 248; (*b*) A. Escuer, R. Vicente, S. B. Kumar, X. Solans, M. Font-Bardia and A. Caneschi, *Inorg. Chem.*, 1996, **35**, 3094; (*c*) X.-M. Chen, Q.-Y. Deng, G. Wang and Y.-J. Xu, *Polyhedron*, 1994, **13**, 3085; (*d*) P. E. Kruger, G. D. Fallon, B. Moubaraki, K. J. Berry and K. S. Murray, *Inorg. Chem.*, 1995, **33**, 4808.
37 P. Zuman and R. Patel, *Techniques in Organic Reaction Kinetics*, Wiley, New York, 1984, p. 296; H. Strehlow, *Rapid Reactions in Solution*, VCH, Weinheim, 1992, p. 103.
38 R. Menif, J. Reibenspies and A. E. Martell, *Inorg. Chem.*, 1991, **30**, 3446.
39 F. Meyer and P. Rutsch, *Chem. Commun.*, 1998, 1037.
40 Z.-W. Mao, G. Liehr and R. van Eldik, *J. Am. Chem. Soc.*, 2000, **122**, 4839.